Interference of Sulphur Dioxide on Balloon-borne Electrochemical Concentration Cell Ozone Sensors over the Mexico City Metropolitan Area

Isao Kanda*, Roberto Basaldud[1], Nobuji Horikoshi[2], Yukiyo Okazaki, Sandy-Edith Benítez-Garcia[3], Abraham Ortínez[1], Victor Ramos Benítez[4], Beatriz Cárdenas[1] and Shinji Wakamatsu

Ehime University, 3-5-7 Tarumi, Matsuyama, Ehime, Japan
[1]National Institute of Ecology and Climate Change (INECC), Periférico 5000, Col. Insurgentes Cuicuilco,
Delegación Coyoaceán, D.F., Mexico
[2]Meteoric Research Inc., 245-8 Uratakao, Hachiouji, Tokyo, Japan
[3]Department of Life Environment Conservation Science, United Graduate School of Agricultural Sciences, Ehime University,
3-5-7 Tarumi, Matsuyama, Ehime, Japan.
[4]National Weather Service (SMN), Av. Observatorio 192, Col. Observatorio, Del. Miguel Hidalgo, D.F., Mexico

*Corresponding author. Tel: +81-89-946-9851, E-mail: ikanda@agr.ehime-u.ac.jp

ABSTRACT

An abnormal decrease in ozonesonde sensor signal occurred during air-pollution study campaigns in November 2011 and March 2012 in Mexico City Metropolitan Area (MCMA). Sharp drops in sensor signal around 5 km above sea level and above were observed in November 2011, and a reduction of signal over a broad range of altitude was observed in the convective boundary layer in March 2012. Circumstantial evidence indicated that SO_2 gas interfered with the electrochemical concentration cell (ECC) ozone sensors in the ozonesonde and that this interference was the cause of the reduced sensor signal output. The sharp drops in November 2011 were attributed to the SO_2 plume from Popocatépetl volcano southeast of MCMA. Experiments on the response of the ECC sensor to representative atmospheric trace gases showed that only SO_2 could cause the observed abrupt drops in sensor signal. The vertical profile of the plume reproduced by a Lagrangian particle diffusion simulation supported this finding. A near-ground reduction in the sensor signal in March 2012 was attributed to an SO_2 plume from the Tula industrial complex north-west of MCMA. Before and at the time of ozonesonde launch, intermittent high SO_2 concentrations were recorded at ground-level monitoring stations north of MCMA. The difference between the O_3 concentration measured by the ozonesonde and that recorded by a UV-based O_3 monitor was consistent with the SO_2 concentration recorded by a UV-based monitor on the ground. The vertical profiles of the plumes estimated by Lagrangian particle diffusion simulation agreed fairly well with the observed profile. Statistical analysis of the wind field in MCMA revealed that the effect Popocatépetl was most likely to have occurred from June to October, whereas the effect of the industries north of MCMA, including the Tula complex, was predicted to occur throughout the year.

Key words: Electrochemical concentration cell, Mexico City, Ozone, Ozonesonde, Sulphur dioxide

1. INTRODUCTION

In 1992, Mexico City had among the worst air quality of any megacity in the world (Mage *et al.*, 1996). Although the overall level of ozone (O_3) in Mexico City has decreased substantially since 1992, present-day concentrations of O_3 in Mexico City frequently exceed the current Mexican environmental standard for O_3 (hourly average, 110 ppb; 8-h average, 80 ppb).

Many authors (e.g., Molina *et al.*, 2010; Velasco *et al.*, 2008) studied the production, transport, chemical reactions, and desctruction of O_3 in Mexico City and in the Mexico City Metropolitan Area (MCMA) (Fig. 1). In our research, we used an ozonesonde to obtain vertical profiles of O_3 twice daily to elucidate the mechanism of formation of O_3 in MCMA.

To measure the concentration of O_3, we used the electrochemical concentration cell (ECC) ozone sensor originally developed by Komhyr (1969). The relability of the ECC ozone sensor has been confirmed in many studies [e.g., Komhyr *et al.* (1995) and Barnes and Bandy (1985)]; however, the ECC sensor is known to be affected by the presence of sulphur dioxide (SO_2).
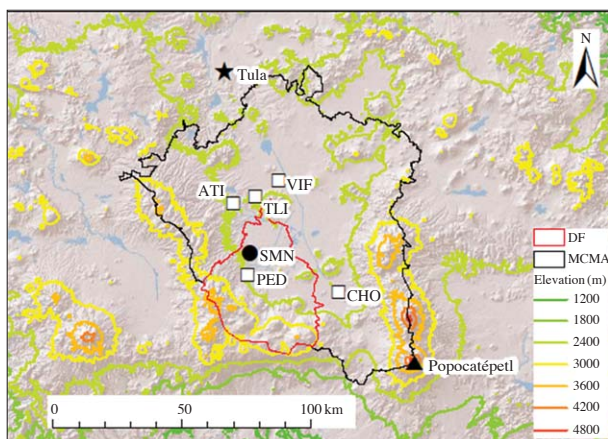
Fig. 1. Map of the Mexico City Metropolitan Area (MCMA). The region denoted by DF is the Federal District. The black circle is the SMN balloon launching site, and the white squares are stations of the Mexico City air-monitoring network (RAMA): VIF, Villa de las Flores; PED, Pedregal; CHO, Chalco; TLI, Tultitlan; ATI, Atizapan.

Flentje *et al.* (2010) reported a clear effect of SO_2 on ozonesonde measurements in continental Europe during the eruption of Eyjafjallajökull, Iceland, in April 2010. To compensate for the effect of SO_2, Morris *et al.* (2010) used tandem ozonesondes, one with an SO_2 filter and the other without, to simultaneously determine vertical profiles of O_3 and SO_2 in the presence of industrial (Houston, TX, USA), and volcanic (Sapporo, Japan) SO_2 plumes.

The Tula industrial complex and Popocatépetl volcano are the two main sources of SO_2 emissions around MCMA. The Tula complex has an oil refinery and an electric power plant. Popocatépetl is an active stratovolcano, erupting with increased frequency in recent years. The impact of these SO_2 sources on the air-quality of MCMA was analysed by de Foy *et al.* (2009) using ground-based monitoring equipment, wind profilers, satellite remote sensing, and a numerical chemical transport model. They identified frequent ground-level high-SO_2-concentration incidents attributable to SO_2 emissions from the Tula complex and less frequent incidents attributable to SO_2 emissions from Popocatépetl. However, their analysis of the contribution of SO_2 from Popocatépetl relied heavily on a chemical transport model and satellite remote sensing, the former having considerable uncertainty in the complex terrain of MCMA and the latter lacking sufficiently high spatial and temporal resolutions. A similar study was carried out by Almanza *et al.* (2012) using only ground-based monitoring data for comparison. Thus, there have been virtually no studies of the vertical structure of SO_2 plumes from the two sources compa-

rable to the studies by Morris *et al.* (2010).

(Ozonesonde data used by Thompson *et al.* (2008) clearly indicate interference by SO_2, but no discussion was provided.)

In our study, ozonesonde measurements (without SO_2 filters) were conducted in November 2011 and March 2012 in MCMA. In some measurements, the ECC ozone sensor gave abnormally low readings. SO_2 plumes from the two major sources around MCMA were considered the most important cause of these low readings among other possibilities such as NO_x plumes from airplanes, ECC sensor failure, and O_3 destruction by volcanic substances. Here, we attempt to clarify the causal relationship by using an atmospheric dispersion model and, by analysing routine radiosonde data, to identify the months when SO_2 interference was expected to be frequent.

2. PRELIMINARIES

2.1 ECC Ozone Sensor

The ECC ozone sensor consists of anode and cathode cells: the cathode cell contains buffered 0.5% KI solution, and the anode cell contains saturated KI solution. The ambient O_3 is pumped at a specified flow rate into the cathode cell where O_3 reacts with iodide ion (I^-) as

$$O_3 + 2H^+ + 2I^- \rightarrow I_2 + H_2O + O_2 \qquad (R1)$$
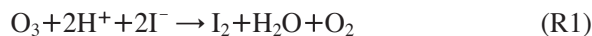
Iodide ion from the anode flows through the ion bridge that connects the cathode and anode cells, and electrons flow through the platinum electrodes at the bottom of the cells, to re-establish charge balance. The measured electric current is therefore proportional to the rate of influx of O_3 molecules (Komhyr, 1969).

If SO_2 is present in the ambient air, the cathode-cell reaction is modified as follows (Schenkel and Broder, 1982). First, the dissolved SO_2 dissociates into HSO_3^- and SO_3^{2-}:

$$SO_2 + H_2O \rightleftharpoons HSO_3^- + H^+$$
$$HSO_3^- \rightleftharpoons SO_3^{2-} + H^+$$
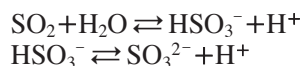
At pH 7, the aqueous concentrations of HSO_3^- and SO_3^{2-} are approximately the same (Seinfeld and Pandis, 2006). Then, the dissolved O_3 reacts preferentially with S (IV) species rather than with I^-.

$$O_3 + HSO_3^- \rightarrow SO_4^{2-} + O_2 + H^+$$
$$O_3 + SO_3^{2-} \rightarrow SO_4^{2-} + O_2$$
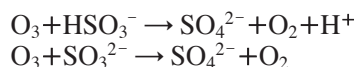
Because these reactions do not induce electric current through the electrodes, the current that would have resulted from the iodide-ozone reaction is lost. In other

words, 1 molecule of SO_2 is measured as -1 molecule of O_3. If there are more SO_2 molecules than O_3 molecules, the unreacted HSO_3^- and SO_3^{2-} remains in the aqueous phase until all of the SO_2 is consumed by later incoming O_3. In the measurement, this means that the zero signal continues until all of the dissolved SO_2 is consumed. As explained by Schenkel and Broder (1982), reaction of O_3 with the dissolved forms of NO_x is not preferred over that with I^-.

To prevent the SO_2 interference, a strong oxidizing agent is used to filter out SO_2 in KI-based O_3 monitors. Morris *et al.* (2010) demonstrated application of a CrO_3-based SO_2 filter to ECC ozone sensors. Using two ECC sensors in tandem, one with the SO_2 filter and the other without, they could measure O_3 and SO_2 concentrations simultaneously. In our observation campaigns, we did not apply the SO_2 filter because at the time of campaign planning we were not aware of the SO_2 interference or the filtering technology.

A property of an ECC sensor that is helpful in interpreting the observed signal is the response time to a sudden change of input-gas composition. We conducted a laboratory experiment in which the input gas was switched between ozone-free air and ozone-containing air (about 160 ppb O_3). For eight ECC sensors, the output current fitted approximately to exponential forms

$$I = I_b + (I_0 - I_b)(1 - \exp(-t/\tau_r)) \quad \text{(rise response),} \quad (1)$$

$$I = I_b + (I_0 - I_b)\exp(-t/\tau_d) \quad \text{(decay response),} \quad (2)$$

where $I_0 = 5.0\ \mu A$ is the ECC output for the ozone-containing air, $I_b = 0.3\ \mu A$ is the background current for the ozone-free air, and the time constants for the rise and decay responses are $\tau_r \approx 22$ s and $\tau_d \approx 21$ s, respectively.

Fig. 2 shows the response of the ECC sensor when the input gas was changed from ozone-containing air (about 160 ppb O_3) to various gases: ozone-free air, air containing 200 ppb SO_2, air containing 200 ppb NO, and air containing a mixture of 200 ppb NO and 150 ppb O_3. The 200 ppb NO + 150 ppb O_3 mixture was used to determine the response to NO_2 (NO_2 results from reaction of NO with O_3). Because SO_2 dissolves quickly into the KI solution in the ECC sensor and prevents residual O_3 from reacting with I^-, the response of the sensor to SO_2 was much faster than its response to other gases.

2.2 SO₂ Emission Sources

The primary sources of SO_2 emission in the Tula industrial complex (20° 03′N, 99° 17′W about 70 km north-west of the Servicio Meteorológico Nacional (SMN) observation site; Fig. 1) are the Miguel Hidalgo oil refinery (76 kton/year; INEM, 2008) and the Fran-
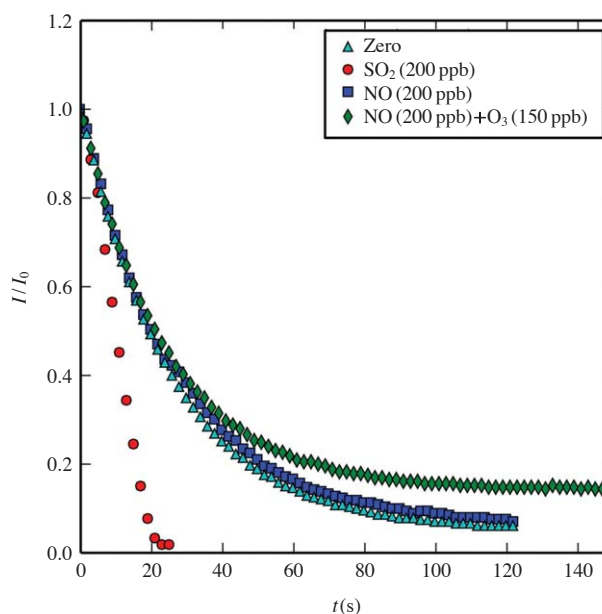

Fig. 2. Response of the ECC ozone sensor when the input gas was changed abruptly from ozone-containing air (≈ 160 ppb O_3) to various gases indicated in the legend. "Zero" represents air filtered through activated carbon to remove ozone.

cisco Pérez Ríos power plant (136 kton/year; INEM, 2008). In contrast, the amount of SO_2 emitted in the Federal District (the core area of MCMA) is 2.8 kton/ year (INEM, 2008), of which about 2.0 kton/year is from mobile sources. Hence, the amount of SO_2 emitted in the Federal District is only about 1.3% of the combined amount of SO_2 emitted from the refinery and power plant in the Tula complex.

SO_2 emissions from the Tula complex are not steady, and the ambient SO_2 concentrations measured at the monitoring stations in the northern part of MCMA show irregular intermittent peaks often reaching as high as 300 ppb. Fig. 3 shows histograms of hourly SO_2 concentrations at the Villa de las Flores (VIF), Pedregal (PED), and Chalco (CHO) monitoring stations (see Fig. 1) in the RAMA (Spanish acronym for automatic atmosphere monitoring network) network for the period from 1 January to 31 December 2011. We observe that the frequency of high concentration increases as the station becomes closer to the Tula complex.

Popocatépetl (5426 m above sea level (ASL), 19° 01′ 20″N, 98° 37′40″W; Fig. 1) is an active strato-volcano located about 70 km southeast of SMN. Except for an ash emission in 1994, the volcano was dormant from 1927 to 1994. However, since December 2000, when large eruptions occurred, Popocatépetl has been degassing continuously and erupting sporadically. On the basis of differential optical absorption spectrometry
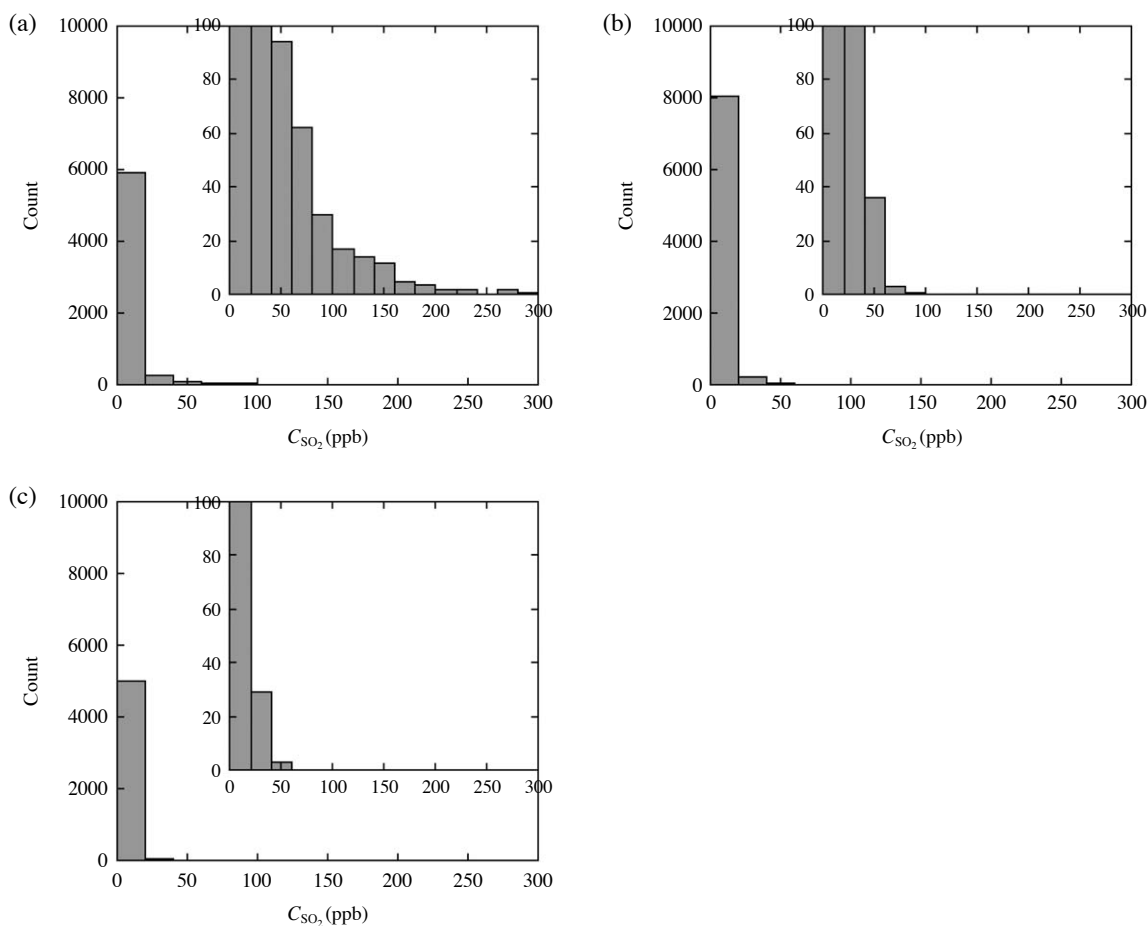
Fig. 3. Histograms of hourly SO_2 concentrations at the VIF (a), PED (b), and CHO (c) stations (see Fig. 1) from 1 January to 31 December 2011.

measurements in March 2006, Grutter *et al.* (2008) estimated the rate of SO_2 emission to be 2.45 ± 1.39 (894 ± 507 kton/year). Although the estimated rate of SO_2 emission is considerably larger than that from the anthropogenic sources, the contribution to the ground-level concentration is relatively small because the height of emission is above or approximately equal to the top of the convective boundary layer. Using numerical meteorological models, de Foy *et al.* (2009) estimated the contribution at 3%-18% in March 2006 when the MILAGRO campaign was conducted.

2.3 Ozonesonde Measurements

With the aim of determining the vertical profile of O_3 in MCMA, we carried out ozonesonde measurements in November 2011 and March 2012. The balloon launch site was the rooftop of the SMN building (2313 m ASL, 19°24′13″N, 99°11′46″W, WMO station index 76680) where routine atmospheric sounding is conducted twice daily at 00Z and 12Z [18:00

and 06:00 LST (local standard time)]. The observation dates were 17, 22, and 23 November 2011, and 7, 8, 9, 12, 13, and 14 March 2012. On each day, a GPS (global positioning system) radiosonde (Meisei Electric Co. Ltd., Japan) was launched at 08:30 and 17:30 LST, and an ozonesonde [GPS radiosonde+ECC O_3 sensor (EnSci Co., U.S.A.)] was launched at 11:30 and 14:30 LST. The actual balloon launch times were often later than these nominal times by up to 30 min. The ascending speed of the observation balloons was set at about $5\,\mathrm{ms^{-1}}$, and data were recorded up to about 15 km for the GPS radiosonde and 30 km for the ozonesonde until the balloon burst. In this paper, we present results up to 8 km ASL below which SO_2 interferes with the ECC sensor. Results at higher altitudes and characteristics of O_3 profiles will be presented elsewhere.

At the launch site, we installed an O_3 monitor based on UV absorption (OA-781, Kimoto Electric, Japan) for all observation periods and an SO_2 monitor based

on UV absorption (Model 43C, Thermo Scientific, U.S.A.) for observation dates 12-14 March 2012. These monitors recorded ground-level ambient concentrations.

3. SO$_2$ INTERFERENCE EVENTS

3.1 Popocatépetl Emission

During the campaign of November 2011, we observed frequent sudden drops in the ECC sensor output at about 5 km ASL: one or two sharp minima for the launches at 14:30 LST on 17 November (Fig. 4b), 11:30 LST on 22 November (Fig. 4c), and 11:30 LST on 23 November (Fig. 4e), and a 1.5-km-thick layer of zero signal for the launch at 14:30 LST on 22 November 22 (Fig. 4d). On two occasions (Fig. 4a and 4f), the ECC sensor signal change was gradual, which was considered to represent a typical transition from the mixing layer to the free troposphere.

Outside the region where minima occurred, the magnitude and fluctuation of the signal were normal, and the ground-level concentration of O$_3$ measured by the ECC sensor agreed well with that measured by the UV-based equipment. The range of the sounding profiles can be regarded as the vertical profiles at SMN because the horizontal distance travelled by the balloons during their ascent to 8 km ASL was at most 7 km from SMN.

The sudden changes in the ECC sensor signal cannot be explained by sudden changes in the ambient O$_3$ concentration. The dashed lines in Fig. 4 indicate the response of the ECC sensor if the ambient O$_3$ partial pressure dropped abruptly to zero from the values at the bottom of the curves. Note that the amount of ozone is represented by its partial pressure so that the response curves across layers with different ambient pressures can be easily compared. Except for the cases on 23 November 2011 (Fig. 4e and 4f), changes in predicted response curves are more gradual than those in the observed curves. The sharp drops observed in Fig. 4b, 4c, and 4d could not have occurred if there was a layer depleted of O$_3$ without any other substances that interfered with the ECC sensor. We note that Morris *et al.* (2010), who used two ozonesondes one with an SO$_2$ filter and the other without, found no particular O$_3$ defect at the height where a sharp SO$_2$ peak, which was attributed to a volcanic plume, was recorded.

A probable cause for the sudden drops in the ECC sensor signal is SO$_2$ plumes from Popocatépetl. As described in Sect. 2.1, the sensor output is reduced at a much faster rate in the presence of SO$_2$ than in the presence of the other gases tested, including ozone-free air.

The summit crater of Popocatépetl is at about the same height as that at which the signal dropped. During the observation campaign, Popocatépetl was relatively active, with a large eruption on November 20. Our sounding results indicated that the wind was generally from the south-east around the height of the summit of Popocatépetl and the SO$_2$ emitted from Popocatépetl could have been advected toward SMN.

Emission of NO$_x$ from airplanes was a concern because flights arriving at and departing from Mexico City International Airport pass over SMN frequently (every few minutes). However, as demonstrated by Schenkel and Broder (1982) and by our experiments (Fig. 2), the effect of NO$_x$ on the ECC ozone sensor is negligible. Ozone depletion due to substances contained in the volcanic gas could have contributed to the decrease in the signal. However, as mentioned previously in relation to Fig. 4, there must have been some other cause for the rapid signal drops. Another possible cause for the signal drops is temporary clogging of the ECC sensor inlet by ice particles. However, how such clogging caused the signal drops is not clear; in a laboratory test, simply closing the inlet by finger was found to reverse the airflow and make the KI solution in the cathode cell flow back to the pump.

From Fig. 4d, one can infer either that the SO$_2$ plume had a thickness of about 1.5 km or that the concentration of SO$_2$ was higher than the concentration of O$_3$ at a certain height so that zero signal continued until the residual SO$_2$ in the reaction cell was consumed. Whether the SO$_2$ plume could have a thickness comparable to that of the affected layer ($\approx$1.5 km) is examined later by numerical simulation. We note here that because the wind speed at the summit of Popocatépetl was in the range 5-10 ms^{-1}, the time required for an air parcel to travel from Popocatépetl to SMN was 2-4 h. No large eruption occurred on 22 November, so the plume should have been due to passive degassing from the crater.

For the cases where the signal did not reach zero, the signal profiles indicate the vertical structures of the SO$_2$ plumes. However, the profiles do not necessarily indicate the dominant thickness of the plumes because the observation balloons could have moved through fringe regions of the plumes. For the same reason and also because the rate of emission of SO$_2$ from Popocatépetl is unknown, the overall concentration field of the SO$_2$ plumes is difficult to estimate only from the observed signals. Despite these limitations, we can at least say from Fig. 4 that the plume thickness was larger than a few hundred metres.

### 3.2 Numerical Simulation of the Popocatépetl Plume

We numerically simulated the thickness of the Popo-
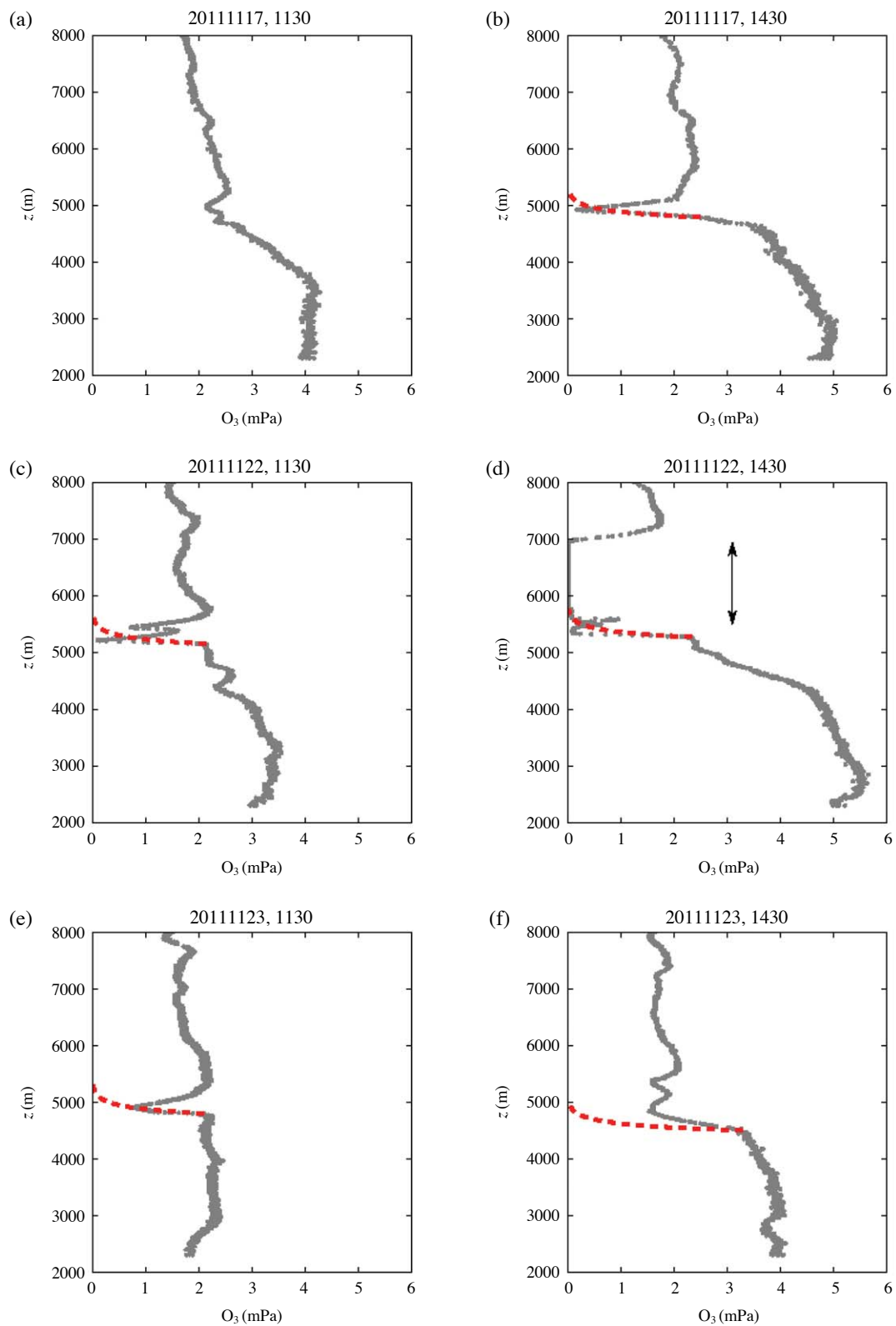
Fig. 4. Vertical profiles of the partial pressure of O_3 during the campaign in November 2011. The nominal launch times are LST. The height z is ASL. The dashed lines indicate expected responses of the ECC ozone sensor if the O_3 concentration dropped abruptly to zero at the height corresponding to the bottom of the curves.

catépetl SO_2 plume by using WRF (Weather Research and Forecasting) version 3.3.1 (Skamarock *et al.*, 2008) and FLEXPART (Stohl *et al.*, 2005) modified to work with WRF outputs (Fast and Easter, 2006). Salient conditions of the simulation were as follows. In the WRF simulation, a single domain was defined around Popocatépetl with $288 \times 186 \times 32$ grids of 3×3 km horizontal size. The thickness of the 32 vertical layers increased from 26 m at the bottom to about 600 m at ≈ 3 km AGL up to the domain top at 16 km ASL. The input meteorological data were NCEP (National Centers for Environmental Prediction) final reanalysis (FNL) data with $1° \times 1°$ horizontal resolution and 6-h time interval. The spatial resolution of the terrain data was 30 s. The sub-models employed were the WSM (WRF Single Moment) 6-class model for cloud microphysics, the MM5 Monin-Obukhov model for the surface boundary layer, the Yonsei University model for the planetary boundary layer, and the unified Noah model for the land surface. Because the FNL data did not resolve the fine structure of the wind field obtained by our sounding results, observation nudging was applied to the whole domain using our sounding data collected four times daily. Grid nudging (typical data assimilation technique when additional observation data are not available) was also applied at the times
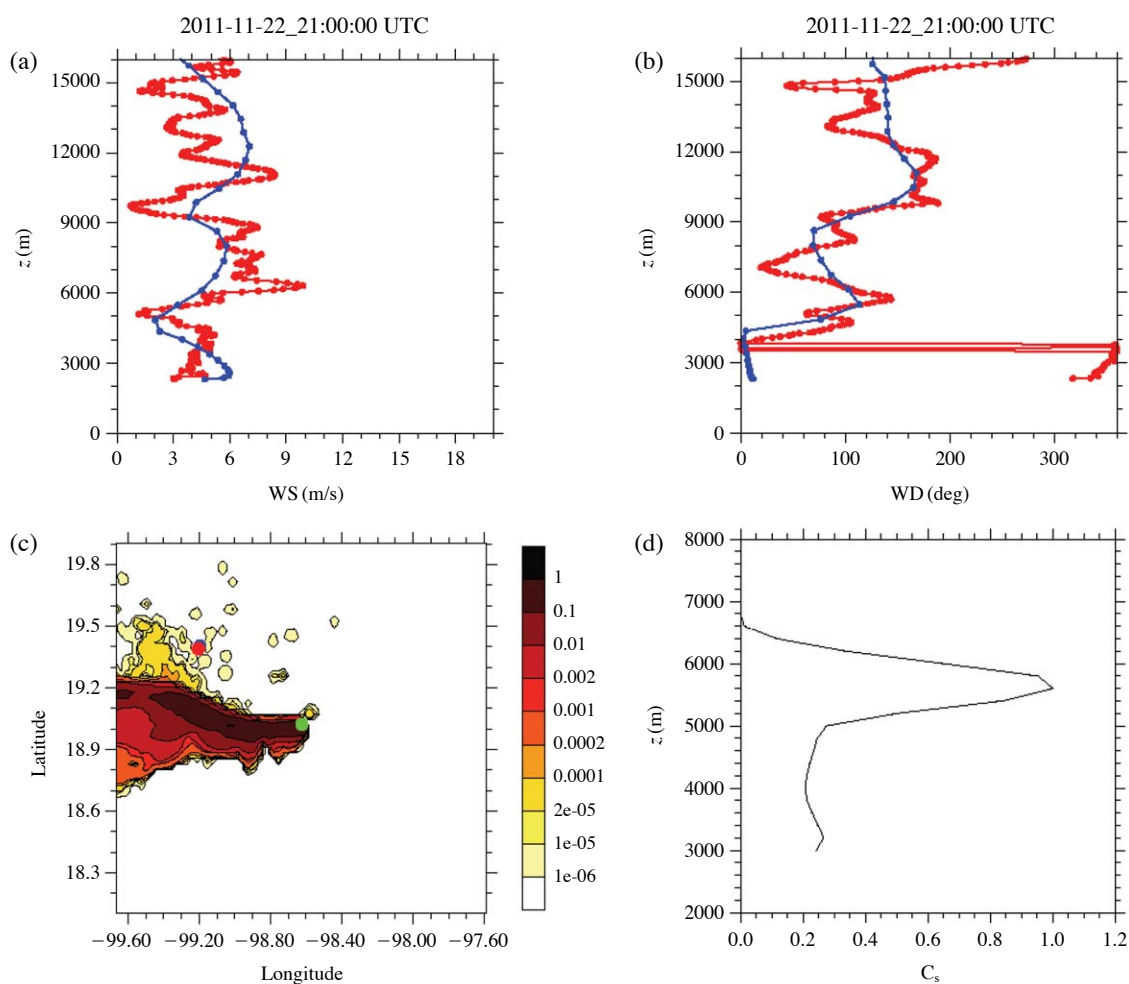
Fig. 5. Results of WRF+FLEXPART numerical simulation for 15:00 LST (21:00 UTC) on 22 November 2011. The height z is ASL. (a, b) Vertical profiles of wind speed and wind direction (blue, WRF; red, observation). (c) Forward particle release simulation by FLEXPART. One million particles totalling a unit mass were released from the summit of Popocatépetl for 20 h beginning at 19:00 LST on 21 November 2011. The release height was between 5426 m ASL (summit) and 5926 m ASL. The contours represent the concentration (m^{-3}) in the horizontal section at 5500 m ASL. The coordinate values (in degrees) are longitude (positive in the east) and latitude (positive in the north). The red and green circles indicate the locations of SMN and the Popocatépetl summit, respectively. (d) Vertical profile of the number of particles concentrically located 60 to 80 km from the centre of Popocatépetl. The particle number C_s is normalized by the maximum value at 5500 m ASL.

when FNL data were available. These nudging proce-
dures in effect introduced non-physical forcing to the
governing equations in the whole domain well beyond
the valid range of the sounding results, but for the
current purpose of reproducing the approximate SO_2
plume, this rather crude method is justified. The WRF
simulation was run for 48 h from 00:00 LST on 21
November 2011, the first 24 h considered as a spin-up
period.

The Lagrangian stochastic model FLEXPART was
employed because the steep terrain near Popocatépetl
would induce substantial numerical diffusion if an Eul-
erian diffusion model were used. The wind field deri-
ves from the WRF simulation saved at 1-h intervals.
Above the Popocatépetl crater at an elevation between
5426 m ASL (summit) and 5926 m ASL, a total of 1
million particles were released randomly for 20 h start-
ing at 19:00 LST on 21 November 2011. The chosen
elevation range is a crude guess from the infrared side-
view of Popocatépetl in Grutter *et al.* (2008). Note
that it was not feasible to estimate the rate of emission
of SO_2 from Popocatépetl based on Grutter *et al.* (2008),
who reported an order-of-magnitude variation in SO_2
column amount during a single month, or based on
satellite data [e.g., data from the Ozone Monitoring
Instrument, which passed over MCMA only once (aro-
und 20:00 LST on 23 November 2011) during the ob-
servation period].

Fig. 5 compares WRF simulation results for wind
speed (Fig. 5a) and wind direction (Fig. 5b) with our
sounding results for 15:00 LST (21:00 UTC) on 22
November 2011. We observe that the east-to-south-
east wind around 6000 m ASL is simulated fairly well.
Note that, without observation nudging, the wind direc-
tion variation at 4000-8000 m could not be reproduced
by WRF simulation, and the simulated wind was almost
uniformly from the east.

Fig. 5c shows particle concentration contours at 5500
m ASL for 15:00 LST (21:00 UTC) on 22 November
2011. The red circle indicates the location of SMN.
On the scale of Fig. 5c, the horizontal locations of
SMN and the observation balloon at 5500 m are almost
coincident. The majority of the plume was transported
primarily towards the west, but a portion was carried
to the north-west where SMN is located. As shown in
Fig. 5b, the observed wind had a more south-easterly
component, and the real plume should have been bent
further towards the north than shown in Fig. 5c.

Fig. 5d shows the vertical profile of the number of
particles concentrically located 60 to 80 km from the
centre of Popocatépetl. The number of particles was
normalized by the maximum value around 5500 m
ASL. The profile indicates that the plume thickness
was about 1 km. The calculated thickness was almost

the same for other times and under simulation condi-
tions (e.g., different release height) not considerably
different from those of the presented case. The case
shown in Fig. 4d, corresponding to the simulation time
in Fig. 5, can be interpreted as follows: either the sound-
ing balloon transected a thick portion of the plume, or
the balloon met a thin dense SO_2 portion of the plume
and SO_2 continuously interfered with the ECC sensor
until all of the dissolved SO_2 molecules were consum-
ed. In the other cases in Fig. 4, the balloons may have
traversed thin fringe portions of the plume.

3.3 Tula Emission

On 14 March 2012, the ozonesonde scheduled for
launch at 11:30 LST gave a considerably lower read-
ing of O_3 concentration ($\approx$33 ppb) than did the UV-bas-
ed equipment ($\approx$53 ppb). As shown in Fig. 6, the verti-
cal profile of O_3 concentration had a considerably thic-
ker layer with reduced O_3 than that would have been
caused only by decomposition on solid surfaces and
reaction with NO near the ground. The ground-level
O_3 concentration on 14 March 2012 was relatively low,
with an afternoon maximum of about 65 ppb. Other-
wise, meteorological conditions on 14 March 2012
were unremarkable.
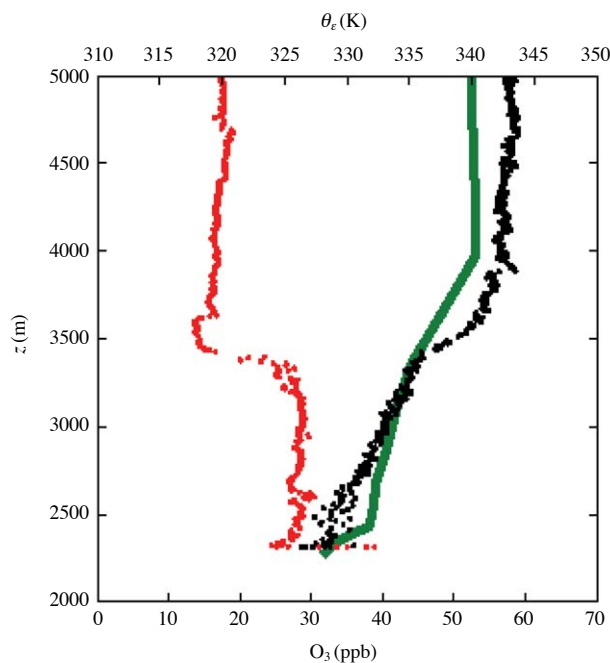
Fig. 6. Vertical distribution of O_3 concentration and equiva-
lent potential temperature for the 11:30 LST launch on 14
March 2012. Black dots, O_3 concentration; red dots, equiva-
lent potential temperature; green curve, influence of the SO_2
plume on O_3 concentration (average of 11:00 and 12:00 LST
results simulated by WRF-FLEXPART).
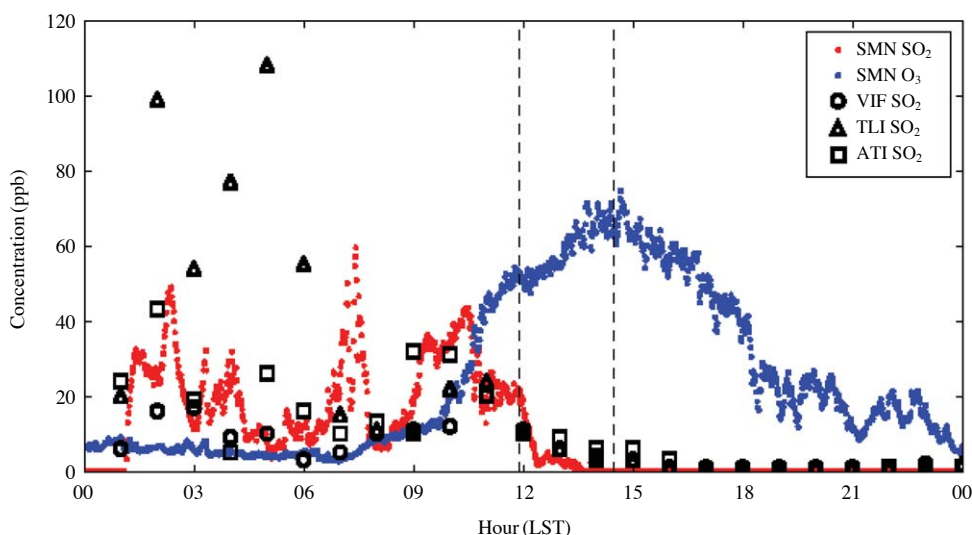
Fig. 7. Trends of O_3 and SO_2 concentrations measured by UV-based equipment at SMN, and SO_2 monitoring data at the VIF, TLI, and ATI air-monitoring stations in the northern part of MCMA on 14 March 2012.

Circumstantial evidence suggested that the low O_3 reading of the ozonesonde on 14 March 2012 was due to the SO_2 plume from the Tula industrial complex. Fig. 7 shows the SO_2 and O_3 concentrations measured on 14 March 2012 by the UV-based equipment at SMN and at monitoring stations in the northern part of MCMA (see Fig. 1). From the wee hours of the morning to shortly after the 11:30 launch, the SO_2 monitor recorded sporadic high SO_2 concentrations. At the time of balloon release (11:30 is a nominal time; the actual release time was 11:54), the SO_2 concentration was about 21 ppb, approximately the difference between the values of the SO_2 concentrations measured by the ozonesonde and the UV-based O_3 monitor. The wind at SMN was from the north in the morning hours, and the SO_2 concentration in the north-western part of MCMA was generally higher than usual and higher than in other parts of the city. The Vallejo district about 7 km north of SMN is also a major emission source of SO_2 because of illegal use of low-grade fuel, but all three air-monitoring stations [ATI (Atizapan), TLI (Tultitlan), and VIF; see Fig. 1] in the northern part of the Vallejo district recorded sporadic high SO_2 concentration at the same time (Fig. 7). In addition, on 14 March 2012, the wind at the VIF station was from the north-north-west on average, with relatively small fluctuations (recorded wind direction: 332°, 304°, 336°, 355°, 27°, 27°, 317°, 13°, 337°, 343°, and 327° from 01:00 to 11:00, respectively). Therefore, it is unlikely that the sporadic high SO_2 concentrations were due to the industry around the Vallejo district.

We remark that the plume of NOx from the Tula complex, northern industry, or local vehicular traffic could not have caused the wide defect of the ECC signal near the ground. Estimated emission rate of NO_x is 24 kton/year from the Tula complex and 146 kton/year from the mobile sources in the Federal District (INEM, 2008). Because the morning rush-hour peaks of NO_x concentration at air-monitoring stations in the north of SMN on 14 March 2012 was not particularly different from those on ordinary weekdays, the local vehicular traffic was the major source of NO_x at SMN. Therefore, ozone depletion by NO titration should have been limited to a shallow layer near the ground. Even if substantial NO titration had occurred, it should have been detected by the UV-based O_3 monitor at SMN.

3.4 Numerical Simulation of the Tula Plume

An instantaneous plume was simulated by WRF+ FLEXPART employing the grid and observation nudging described in Sect. 3.2. The effective stack height of the Tula emissions was estimated to be in the range 400-1430 m by substituting the properties of the individual stacks provided in INEM 2008 into the CONCAWE (Conservation of Clean Air and Water in Western Europe) relation (Brummage, 1968). Then, in a height range between 100 and 1000 m above ground level (AGL), 1 million particles were released randomly for 20 h starting at 19:00 LST on 13 March 2012. Fig. 8 shows concentration contours at 2500 m ASL. The simulated plume traveled primarily toward the south, although the observed surface SO_2 distribution at the RAMA stations plume advancement toward
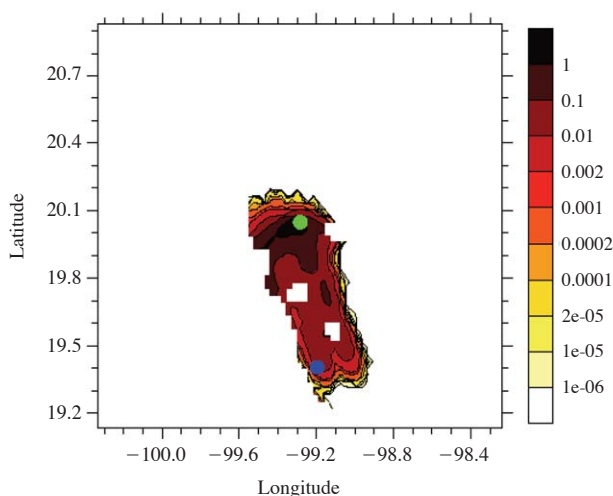
Fig. 8. Result of WRF+FLEXPART numerical simulation for 12:00 LST (18:00 UTC) on 14 March 2012. One million particles totalling a unit mass were released from the Tula industrial complex (green circle) for 20 h beginning at 01:00 UTC on 14 March 2012. The release height was between 100 and 1000 m AGL. The contours represent the concentration in the horizontal section at 2500 m ASL. The white defect cells indicate terrain above 2500 m ASL. The coordinate values (in degrees) are longitude (positive in the east) and latitude (positive in the north). The blue circle indicates the location of SMN.

the south-east (not shown). Note that the plume travelled mainly to the west if observation nudging based on our sounding results was not employed. Because the ECC sensor detects the presence of 1 SO_2 molecule as the absence of 1 O_3 molecule, when the ground-level SO_2 concentration is 21 ppb and the O_3 concentration is 53 ppb, the output signal C_{ECC} of the ECC sensor becomes

$$C_{ECC} = 53 - 21 \frac{C_{SO_2}(z)}{C_{SO_2}(z_G)}, \qquad (3)$$

where z_G is the ASL height of the ground. Values from the calculated vertical profile of SO_2 concentration normalized by the ground-level value at SMN (average of 11:00 and 12:00 LST results) were substituted into Eq.(3). The calculated profile of C_{ECC} (thick green line in Fig. 6) agrees well with the observation except near the ground where the gradient is a little excessive. The approximate agreement implies that the theoretically predicted evolution of the plume is consistent with the observation when the emission source is assumed to be the Tula complex. We note that a plume simulation using a conventional Gaussian-plume method resulted in a poorer agreement with the observation (not shown), probably because this method cannot

account for the complex evolution of the boundary layer in the morning hours when the plume travelled from the Tula complex to SMN for about 6.5 h.

4. ASSESSMENT OF SO$_2$ INFLUENCE ON OZONESONDE

4.1 Effect of Popocatépetl Plume

We identified the months when the SO_2 plume from Popocatépetl was most likely to interfere with ozonesonde measurements. To accomplish this, we averaged wind vectors measured by routine soundings at 00:00 UTC and 12:00 UTC at altitudes ranging from the Popocatépetl summit to 1000 m above the summit (5426-6426 m ASL). The raw sounding data [Vaisala GPS radiosondes: sounding measurements were made every 2 s (approximately 9-m interval)] were provided by SMN. The directions of the vertically averaged wind vectors were sorted into bins of 16 compass-point directions, and frequency distributions were determined for given time periods. The compilation period was from 2006 to 2010, and months with similar distributions were lumped together. The 00:00 UTC and 12:00 UTC data were averaged together because diurnal variation was relatively weak at the selected altitude range. Fig. 9 shows the resulting wind rose.

The prevailing wind direction is west from November to March; east from June to September; and intermediate between these groups of months (i.e., in May and October). The change in wind direction reflects the alternation of the thermal wind. Because the central MCMA is north-west of Popocatépetl, the ECC ozonesonde would be frequently affected by the Popocatépetl SO_2 plume from June to October when the frequency of south-east wind was high ($\geq 8\%$). Our encounter with the Popocatépetl interference in November (frequency of south-east wind was 3.5% in November) was due to meteorological variability; the wind direction in the upper troposphere was indeed not constant (WSW on 17 November, E on 22 and 23 November), typical of the transition period from the wet to the dry season.

If SO_2 filters (Morris *et al.*, 2010) are to be employed to avoid Popocatépetl interference in future ozonesonde observations, it would be sufficient to use them in the months from June to October.

4.2 Effect of Northern Industries

As described by Whiteman *et al.* (2000), solar heating of the ground and the induced updraft in the Mexico Basin generates relatively weak surface air-flow from the wide orographic opening to the north (see Fig. 1). Therefore, the prevailing wind is from the north in

(a) Jan, Feb, Mar, Apr, Nov, Dec

(b) Jun, Jul, Aug, Sep

(c) May

(d) Oct
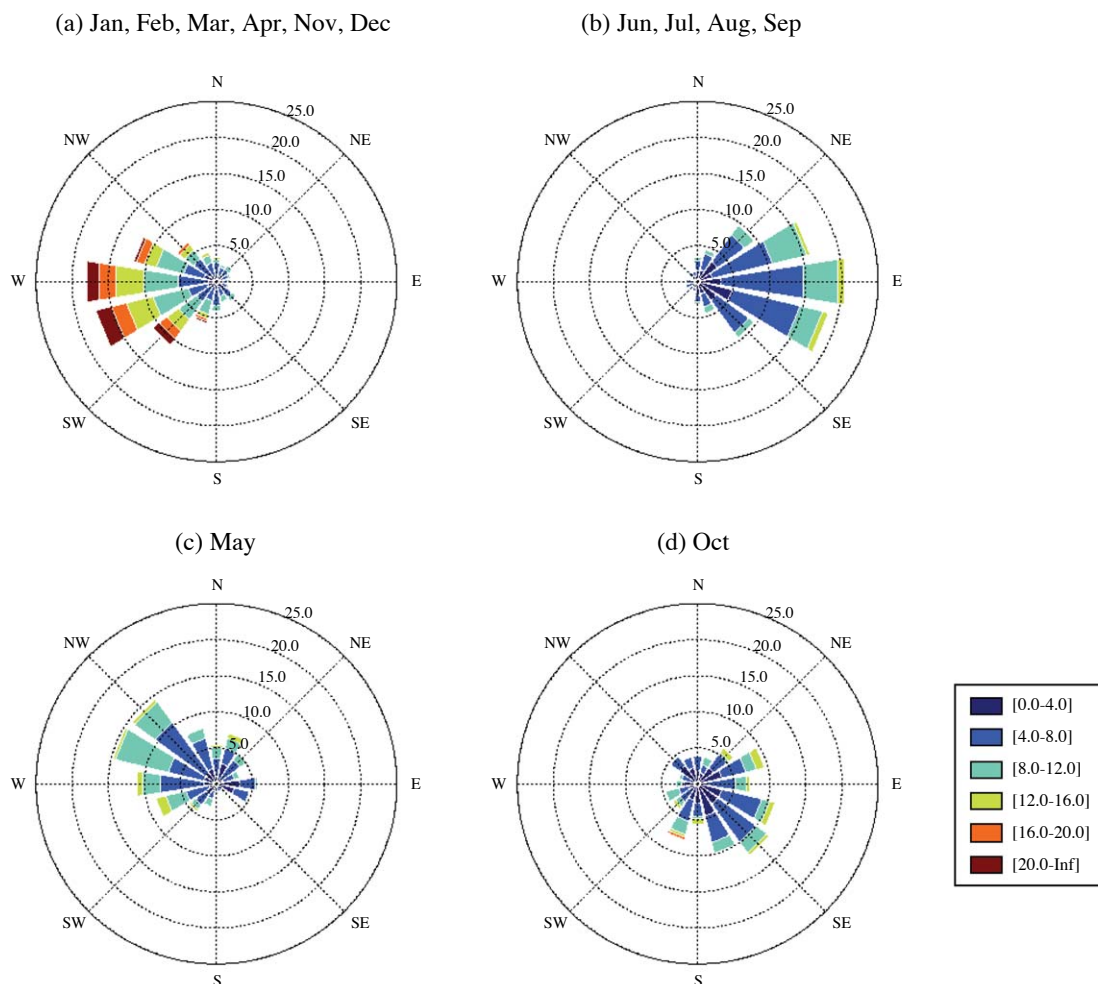
Fig. 9. Wind rose obtained by averaging sounding data at elevations ranging from the Popocatépetl summit to 1000 m above the summit. The unit for wind speed is metres per second and wind-direction frequency is expressed in percent. The data source is routine sounding data collected at SMN from 2006 to 2010. Months with similar distribution are grouped together.

MCMA except in the south-eastern part, where in the afternoon, strong wind enters from the narrow gap of the basin rim in the south-east corner.

Because surface measurements could be influenced by the buildings surrounding SMN, we analysed the average wind direction measured by routine soundings at 2343-2463 m ASL (i.e., up to 150 m AGL, excluding the first 30 m). Fig. 10 shows the averaged wind rose from 2006 to 2010. There were variations from year to year (not shown), but the common characteristic is that the prevailing wind is from the north at 00:00 UTC (18:00 LST) and from the north-west to north-north-west at 12:00 UTC (06:00 LST). Therefore, the wind potentially carries SO_2 emissions from industries in the north, including the Tula complex, to the centre of MCMA. As shown in Fig. 3, high-SO_2-concentration plumes do not occur very frequently in the northern

part of MCMA, but when they do, they almost certainly reach the SMN site and affect ozonesonde measurements. In our measurement campaigns, SO_2 plumes interfered with ozonesonde measurements in 1 in 18 launches.

Therefore, countermeasures should be implemented against SO_2 interference. Such countermeasures include employing SO_2 filters on all ECC sensors, monitoring SO_2 concentration at the launch site to avoid high-SO_2-concentration events, and preventing the sporadic large emissions of SO_2 from the northern industries; the last option would benefit the air quality in MCMA.

5. CONCLUSIONS

In the ozonesonde observations during our atmosph-

(a) 06:00 LST (12:00 UTC)   (b) 18:00 LST (00:00 UTC)
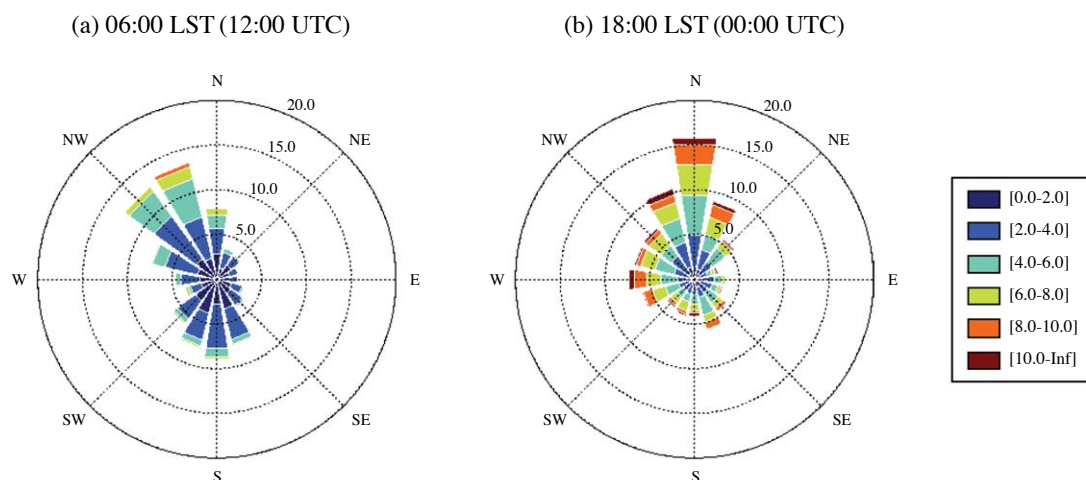
Fig. 10. Wind rose obtained by averaging sounding data at elevations ranging from 2343 to 2463 m ASL (30-150 m AGL at SMN). The unit for wind speed is metres per second and wind-direction frequency is expressed in percent. The data source is routine sounding data collected at SMN from 2006 to 2010.

eric research campaign in MCMA, we found abnormal drops in the ECC sensor signal around and above 5 km or in the convective boundary layer. Analysis of the sensor response time, the emissions inventory, the weather condition, and plume dispersion simulations indicate that the drops in the signal were caused by SO_2 interference by plumes from the Popocatépetl volcano and the Tula industrial complex (14 March 2012). From the analysis of the wind-field statistics in MCMA, we expect that there would be frequent interference by the Popocatépetl plume from June to October and by the Tula plume whenever large emission occurs.

Currently, there are few stations conducting regular ozonesonde measurements in Central America. Because such measurements are vital for curbing local air pollution and addressing the problem of global climate change, regular ozonesonde measurement scheme should be implemented in Mexico in near future. The observations and analysis presented in this paper will be useful in developing strategies for launching ozonesondes.

ACKNOWLEDGEMENT

REFERENCES

Almanza, V.H., Molina, L.T., Sosa, G. (2012) Soot and SO_2 contribution to the supersites in the MILAGRO campaign from elevated flares in the Tula Refinery. Atmospheric Chemistry and Physics 12, 10583-10599.

Barnes, R.A., Bandy, A.R. (1985) Electrochemical concentration cell ozonesonde accuracy and precision. Journal of Geophysical Research 90, 7881-7887.

Brummage, K.G. (1968) The calculation of atmospheric dispersion from a stack. Atmospheric Environment 2, 197-224.

de Foy, B., Krotkov, N.A., Bei, N., Herndon, S.C., Huey, L.G., Martínez, A.-P., Ruiz-Suárez, L.G., Wood, E.C., Zavala, M., Molina, L.T. (2009) Hit from both sides: Tracking industrial and volcanic plumes in Mexico City with surface measurements and OMI SO_2 retrievals during the MILAGRO field campaign. Atmospheric Chemistry and Physics 9, 9599-9617.

Fast, J.D., Easter, R.C. (2006) A Lagrangian particle dispersion model compatible with WRF. 7th Annual WRF User's Workshop, 19-22 June 2006, Boulder, CO, USA.

Flentje, H., Claude, H., Elste, T., Gilge, S., Köhler, U., Plass-Dülmer, C., Steinbrecht, W., Thomas, W., Werner, A., Fricke, W. (2010) The Eyjafjallajökull eruption in April 2010 - detection of volcanic plume using in-situ measurements, ozone sondes and lidar-ceilometer profiles. Atmospheric Chemistry and Physics 10, 10085-

10092.

Grutter, M., Basaldud, R., Rivera, C., Harig, R., Junkerman, W., Caetano, E., Delgado-Granados, H. (2008) SO_2 emissions from Popocatépetl volcano: Emission rates and plume imaging using optical remote sensing techniques. Atmospheric Chemistry and Physics 8, 6655-6663.

INEM (2008) National Inventory of Emissions, Inventario Nacional de Emisiones de Mexico, SEMARNAT-INE, Mexico.

Komhyr, W.D. (1969) Electrochemical cells for gas analysis. Annals of Geophysics 25, 203-210.

Komhyr, W.D., Barnes, R.A., Brothers, G.B., Lathrop, J.A., Opperman, D.P. (1995) Electrochemical concentration cell ozonesonde performance evaluation during STOIC 1989. Journal of Geophysical Research 100, 9231-9244.

Mage, D., Ozolins, G., Peterson, P., Webster, A., Orthofer, R., Vandeweerd, V., Gwynne, M. (1996) Urban air pollution in megacities of the world. Atmospheric Environment 30, 681-686.

Molina, L.T., Modronich, S., Gaffney, J.S., Apel, E., de Foy, B., Fast, J., Ferrare, R., Herndon, S., Jimenez, J.L., Lamb, B., Osornio-Vargas, A.R., Russell, P., Schauer, J.J., Stevens, P.S., Valkamer, R., Zavala, M. (2010) An overview of the MILAGRO 2006 campaign: Mexico City emissions and their transport and transformation, Atmospheric Chemistry and Physics 10, 8697-8760.

Morris, G.A., Komhyr, W.D., Hirokawa, J., Flynn, J., Lefer, B., Krotkov, N., Ngan, F. (2010) A balloon sounding technique for measuring SO_2 plumes. Journal of Atmospheric and Oceanic Technology 27, 1318-1330.

Schenkel, A., Broder, B. (1982) Interference of some trace gases with ozone measurements by the KI method.

Atmospheric Environment 16, 2187-2190.

Seinfeld, J.H., Pandis, S.N. (2006) Atmospheric Chemistry and Physics: From Air Pollution to Climate Change, John Wiley & Sons, Inc., Hoboken, NJ.

Skamarock, W.C., Klemp, J.B., Dudhia, J., Gill, D.O., Barker, D.M., Duda, M.G., Huang, X.-Y., Wang, W., Powers, J.G. (2008) A description of the Advanced Research WRF Version 3, NCAR/TN-475+STR.

Stohl, A., Forster, C., Frank, A., Seibert, P., Wotawa, G. (2005) Technical note: The Lagrangian particle dispersion model FLEXPART version 6.2. Atmospheric Chemistry and Physics 5, 2461-2474.

Thompson, A.M., Yorks, J.E., Miller, S.K., Witte, J.C., Dougherty, K.M., Morris, G.A., Baumgardner, D., Ladino, L., Rappenglück, B. (2008) Tropospheric ozone sources and wave activity over Mexico City and Houston during MILAGRO/Intercontinental Transport Experiment (INTEX-B) Ozonesonde Network Study, 2006 (IONS-06). Atmospheric Chemistry and Physics 8, 5113-5125.

Velasco, E., Márquez, C., Bueno, E., Bernabé, R.M., Sánchez, A., Fentanes, O., Wöhrnschimmel, H., Cárdenas, B., Kamilla, A., Wakamatsu, S., Molina, L.T. (2008) Vertical distribution of ozone and VOCs in the low boundary layer of Mexico City. Atmospheric Chemistry and Physics 8, 3061-3079.

Whiteman, C.D., Zhong, S., Bian, X., Fast, J.D., Doran, J.C. (2000) Boundary layer evolution and regional-scale diurnal circulations over the Mexico Basin and Mexican plateau. Journal of Geophysical Research 105, 10081-10102.